

A multiple model probability hypothesis density tracker for time-lapse cell microscopy sequences

Seyed Hamid Rezatofghi^{1,2}, Stephen Gould¹, Ba-Ngu Vo³,
Katarina Mele², William E. Hughes^{4,5}, and Richard Hartley^{1,6}

¹ College of Engineering & Computer Sci., Australian National University, ACT, AU

² Quantitative Imaging Group, CSIRO Math., Informatics & Statistics, NSW, AU

³ Department of Electrical and Computer Engineering, Curtin University, WA, AU

⁴ The Garvan Institute of Medical Research, NSW, AU

⁵ Department of Medicine, St. Vincent's Hospital, NSW, AU

⁶ National ICT (NICTA), AU

hamid.rezatofghi@anu.edu.au

Abstract. Quantitative analysis of the dynamics of tiny cellular and subcellular structures in time-lapse cell microscopy sequences requires the development of a reliable multi-target tracking method capable of tracking numerous similar targets in the presence of high levels of noise, high target density, maneuvering motion patterns and intricate interactions. The linear Gaussian jump Markov system probability hypothesis density (LGJMS-PHD) filter is a recent Bayesian tracking filter that is well-suited for this task. However, the existing recursion equations for this filter do not consider a state-dependent transition probability matrix. As required in many biological applications, we propose a new closed-form recursion that incorporates this assumption and introduce a general framework for particle tracking using the proposed filter. We apply our scheme to multi-target tracking in total internal reflection fluorescence microscopy (TIRFM) sequences and evaluate the performance of our filter against the existing LGJMS-PHD and IMM-JPDA filters.

1 Introduction

Recent developments in time-lapse cell microscopy imaging systems have had a great impact on the analysis of cellular and intracellular dynamics. However, visual inspection of data acquired by these imaging techniques requires manual tracking of large and time-varying numbers of tiny structures in noisy images. Therefore, automated tracking methods have been extensively used in different biological applications in the last decade [1–9]. Despite significant technical advances made in automatically tracking moving objects, particle tracking remains a challenging task due to the complex nature of biological applications. The microscopic sequences are usually populated with visually similar tiny structures having intricate motion patterns and sophisticated interactions with other structures such as spawning (mitosis) and merging. Moreover, the structures may enter, exit, or temporarily disappear from the field of view or be occluded by other cellular objects. In addition in some imaging techniques, e.g. fluorescence microscopy imaging, the sequences are contaminated with high levels of noise

which complicates detection. Thus for success in biological applications, particle tracking methods should be able to track an unknown and time-varying number of similar structures in the presence of clutter noise and detection uncertainty.

To this end, many tracking approaches have been proposed. Bayesian tracking approaches are a class of probabilistic tracking algorithms that have become popular for many cell tracking applications in recent years [1–9]. These tracking methods can theoretically deal with the aforementioned difficulties by incorporating prior knowledge of object dynamics and measurement models. Recently, a new generation of Bayesian filters based on Random Finite Set (RFS) theory has been proposed in the literature [10, 11]. In this approach, the state of targets and measurements are modeled as random finite sets. Then, the Bayesian filtering framework is used to recursively estimate and update the joint posterior density of the targets’ states as a random finite set. This elegant formulation avoids explicit track management and associations between measurements and targets which makes this approach advantageous compared to the traditional Bayesian tracking algorithms such as Kalman [1–3] and Particle [4–7] filters. Mahler [11] recently proposed a computationally tractable RFS filter which propagates the first statistical moment of the RFS probability density function of targets, the so called Probabilistic Hypothesis Density (PHD). Due to its good performance and significantly low processing time, the filter has been recently used in various applications such as computer vision [12]. In biological applications, we know of only two published applications of this filter to cell tracking [8, 9]. In these papers, the motion of their microscopic structures are modeled using single linear Gaussian dynamics. However, in many biological applications, a single motion model cannot mimic maneuvering dynamics of subcellular structures. Therefore, these approaches cannot be extended to other similar applications.

In this paper, we propose a general framework for tracking cellular and subcellular structures using the multiple model approach or the jump Markov system (JMS) implementation of the PHD filter [13]. To our knowledge, this is the first application of the multiple model approach of the PHD filter to biological imaging. The main contribution of this paper is a new closed-form for the multiple model Gaussian mixture PHD (LGJMS-PHD) filter. As required for biological applications, this new form is more general than the closed-form suggested by Pasha *et al.* [13]. Moreover, since the identity of trajectories is not considered in the PHD filter formulation, we propose a scheme for identity propagation in this filter. To show the efficiency of the proposed framework, we apply it to particle tracking in a specific biological application and compare the tracking results against the results of the existing LGJMS-PHD filter [13] and the IMM-JPDA filter [1], which is the most relevant traditional filter for this task.

2 Background

Let $\mathbf{x}_{k,1}, \dots, \mathbf{x}_{k,N_k}$ and $\mathbf{z}_{k,1}, \dots, \mathbf{z}_{k,M_k}$ be the states of all N_k targets and all M_k measurements at time k , respectively. Over time, some of these targets may disappear, new targets may appear, and the surviving targets evolve to new

states based on their dynamics. Moreover, due to sensor limitations, only some targets are detected at each time step and many measurements are spurious detections (clutter). We can conveniently describe each time slice by two random finite sets, $\mathbf{X}_k = \{\mathbf{x}_{k,1}, \dots, \mathbf{x}_{k,N_k}\}$ and $\mathbf{Z}_k = \{z_{k,1}, \dots, z_{k,M_k}\}$.

In the RFS based Bayesian tracking approach, the goal is to estimate the joint multi-target posterior density of the states at each time step k using the set of all measurements up to this time step. This posterior density, $p(\mathbf{X}_k|\mathbf{Z}_{1:k})$, can be described by a discrete probability distribution and a joint probability density on the targets' cardinality and state, respectively [10]. The Bayesian filtering framework is used to recursively estimate this combinational posterior density using multi-target transition density $f(\mathbf{X}_k|\mathbf{X}_{k-1})$ and multi-target measurement likelihood $g(\mathbf{Z}_k|\mathbf{X}_k)$. Although the filter provides an elegant Bayesian formulation of the multi-target filtering problem, it is computationally intractable [10]. To overcome this problem, Mahler [11] proposed to propagate the probability hypothesis density, or posterior intensity, of the targets $v_k(\mathbf{x})$ which is the first statistical moment of the probability density function $p(\mathbf{X}_k|\mathbf{Z}_{1:k})$. This alleviates the computational burden of the RFS based filter while still using the RFS concept. It has been shown that this posterior intensity can be calculated using the following recursive equations [11],

$$v_{k|k-1}(\mathbf{x}) = \int p_{S,k}(\dot{\mathbf{x}}) f_{k|k-1}(\mathbf{x}|\dot{\mathbf{x}}) v_{k-1}(\dot{\mathbf{x}}) d\dot{\mathbf{x}} + \int \beta_{k|k-1}(\mathbf{x}|\dot{\mathbf{x}}) v_{k-1}(\dot{\mathbf{x}}) d\dot{\mathbf{x}} + \gamma_k(\mathbf{x}), \quad (1)$$

$$v_k(\mathbf{x}) = [1 - p_{D,k}(\mathbf{x})] v_{k|k-1}(\mathbf{x}) + \sum_{z \in \mathbf{Z}_k} \frac{p_{D,k}(\mathbf{x}) g_k(z|\mathbf{x}) v_{k|k-1}(\mathbf{x})}{\kappa_k(z) + \int p_{D,k}(\mathbf{x}) g_k(z|\mathbf{x}) v_{k|k-1}(\mathbf{x}) d\mathbf{x}}, \quad (2)$$

where $p_{S,k}(\cdot)$ and $p_{D,k}(\cdot)$ are survival and detection probabilities, and $\kappa_k(\cdot)$, $\beta_{k|k-1}(\cdot)$ and $\gamma_k(\cdot)$ denote the intensities of clutter, spawn and birth, respectively.

3 Our framework for particle tracking

Since the PHD filter recursion accommodates complexities such as the birth and spawn models, data association uncertainty, clutter noise, and detection uncertainty in its formulation, it is a suitable tracker for many the biological applications. However, this recursion involves integrals and does not have a closed-form solution in general. The Sequential Monte Carlo implementation of this filter, so called SMC-PHD (or particle-PHD) filter [10], is a generic solution for propagating the intensity distribution. However, the drawback of this approach is the high computational cost due to the large number of required particles [14]. In the case where the target dynamics and measurement model are both linear and Gaussian, and the birth and spawn terms can be expressed as a mixture of Gaussians, there is a closed-form for this recursion so called Gaussian mixture PHD (GM-PHD) filter which is computationally efficient [14].

We now tailor a framework using this filter for the complexities of particle tracking in biological applications. To propose a practical tracker for densely populated particles with reasonable processing time, we assume linear Gaussian

models. Moreover, we model maneuvering dynamics of the particles with multiple such models. Although, the JMS multi-target model for the PHD filter was previously proposed by Pasha *et al.* [13], we introduce a more general closed-form implementation.

The state and measurement vectors: Sequences acquired from time-lapse cell microscopy imaging systems usually contain hundreds of cellular structures appearing as similar tiny particles occupying few pixels in the image. Thus, using shape similarity between objects in order to associate the measurements to the tracks may not be helpful. Typically in this approach, the (kinematic) state vector, $\xi \in \mathbb{R}^n$, includes basic features such as position x , velocity \dot{x} , acceleration \ddot{x} , intensity I , and direction ϕ of particles [1–3, 5–9].

The observation (or measurement) vector z contains what can be measured from the sequences, i.e., the intensity of each pixel. However, the intensity of each pixel is usually a non-linear function of the state vector [6, 7]. Therefore in this case, SMC-PHD filter which is computationally intensive, is required for the tracking framework. In contrast, a simple detection approach can be usually applied for calculation of an estimated position \hat{x} or an estimated intensity \hat{I} of each particle. Although the detections may be noisy and include many false alarms, the PHD filter can properly deal with this. Moreover, we can now use the more efficient Gaussian mixture.

Modeling maneuvering behavior of particles: In many biological applications, the cellular structures exhibit intricate motion patterns and maneuvering dynamics which cannot properly described by a single linear Gaussian motion model. Instead, the motions can appropriately model by several linear dynamic models [1–3, 6]. Therefore, we propose a multiple model approach for simulating the motion model of these structures as follows.

For notational convenience, we remove the time index k in our formulation. However, the random variables and intensity distributions are generally time-indexed variables and distributions. All random variables $(\cdot)_k$ at time k and $(\cdot)_{k-1}$ at time $k-1$ are simply shown by (\cdot) and $(\dot{\cdot})$, respectively.

Assume that the maneuvering dynamics of the structures can be properly modeled by \mathcal{M} linear Gaussian models and measurement likelihood has also a linear Gaussian form for each model $r = \{1, \dots, \mathcal{M}\}$ such that $\tilde{f}(\xi|\dot{\xi}, r) = \mathcal{N}(\xi; F(r)\dot{\xi}, Q(r))$ and $g(z|\xi, r) = \mathcal{N}(z; H(r)\xi, R(r))$, where $F(r)$, $H(r)$, $Q(r)$ and $R(r)$ are the transition, the measurement, and the process and measurement noise covariance, matrices for model r , respectively.

In some biological applications [1, 15], the transition from a dynamic model to another model depends not only on the current model but also on the state of the structures, i.e., its position or velocity. Therefore, a more accurate model includes a state-dependent transition probability $t(r|\dot{r}, \dot{\xi})$. Therefore, the transition density $f(\cdot|\cdot)$ for the augmented state vector $\mathbf{x} = (\xi, r)$ can be written as

$$f(\mathbf{x}|\dot{\mathbf{x}}) = \tilde{f}(\xi|\dot{\xi}, r)t(r|\dot{r}, \dot{\xi}) \quad (3)$$

where $\tilde{f}(\cdot|\cdot)$ is the state transition density for a specific model r . In this approach, it is supposed that $t(r|\dot{r}, \dot{\xi})$ can be expressed by an affine mixture of Gaussians,

$$t(r|\acute{r}, \acute{\xi}) = w_t^{(0)}(r, \acute{r}) + \sum_{\tilde{j}=1}^{J_t(r, \acute{r})} w_t^{(\tilde{j})}(r, \acute{r}) \mathcal{N}\left(\acute{\xi}; \mu_t^{(\tilde{j})}(r, \acute{r}), \Sigma_t^{(\tilde{j})}(r, \acute{r})\right), \quad (4)$$

where $w_t^{(j)}, J_t(r, \acute{r}), \mu_t^{(j)}(r, \acute{r})$ and $\Sigma_t^{(j)}(r, \acute{r})$ are given model parameters and are tuned based on prior knowledge about the application. Note $0 \leq t(r|\acute{r}, \acute{\xi}) \leq 1$ and $\sum_r t(r|\acute{r}, \acute{\xi}) = 1, \forall \acute{\xi}, \acute{r}$. The $w_t^{(j)}(\cdot)$ can be negative so that these conditions are met. Instead of having a constant transition probability matrix, the definition $t(\cdot|\cdot)$ as the form of Eq. 4 lets us to adaptively change the transition probability weights $w_t^{(j)}(\cdot)$ based on a set of Gaussian functions of the state $\acute{\xi}$.

Modeling spawn term: Similarly, the state of spawned structures may be affected by the state of their parents in these applications [16]. Therefore, the spawned intensity for the augmented state $\mathbf{x} = (\xi, r)$ is given by

$$\beta(\mathbf{x}|\acute{\mathbf{x}}) = \tilde{\beta}(\xi|\acute{\xi}, \acute{r})\pi(r|\acute{r}, \acute{\xi}), \quad (5)$$

where $\tilde{\beta}(\cdot|\cdot)$ is the spawned intensity of the state ξ for the model r and $\pi(r|\acute{r}, \acute{\xi})$ is the state-dependent spawned transition probability. In this approach, it is assumed that the $\tilde{\beta}(\cdot|\cdot)$ and $\pi(\cdot|\cdot)$ can be represented by a Gaussian mixture and an affine mixture of Gaussians, respectively.

$$\tilde{\beta}(\xi|\acute{\xi}, \acute{r}) = \sum_{\tilde{j}=1}^{J_\beta(\acute{r})} w_\beta^{(\tilde{j})}(\acute{r}) \mathcal{N}\left(\xi; F_\beta^{(\tilde{j})}(\acute{r})\acute{\xi} + d_\beta^{(\tilde{j})}(\acute{r}), Q_\beta^{(\tilde{j})}(\acute{r})\right), \quad (6)$$

$$\pi(r|\acute{r}, \acute{\xi}) = w_\pi^{(0)}(r, \acute{r}) + \sum_{l=1}^{J_\pi(r, \acute{r})} w_\pi^{(l)}(r, \acute{r}) \mathcal{N}\left(\acute{\xi}; \mu_\pi^{(l)}(r, \acute{r}), \Sigma_\pi^{(l)}(r, \acute{r})\right), \quad (7)$$

where $J_\beta(\cdot), w_\beta^{(j)}(\cdot), F_\beta^{(j)}(\cdot), d_\beta^{(j)}(\cdot), Q_\beta^{(j)}(\cdot), J_\pi(\cdot), w_\pi^{(l)}(\cdot), \mu_\pi^{(l)}(\cdot)$ and $\Sigma_\pi^{(l)}(\cdot)$ are given parameters for these models [13] and are set based on a prior knowledge of the spawn phenomena in the application and such that $0 \leq \pi(r|\acute{r}, \acute{\xi}) \leq 1, \forall \acute{\xi}, \acute{r}$. The interpretation for $\pi(\cdot|\cdot)$ is similar to $t(\cdot|\cdot)$ in Eq. 4.

State-dependent survival and detection probabilities: The probabilities that a target survives, $p_{S,k}(\cdot)$, or is detected by the detection scheme, $p_{D,k}(\cdot)$, may depend on its state. For example, the cellular structures may fuse or may disappear from the field of view around specific locations. Similarly, the probability of detection may vary such that the structures with faint intensity may not be detected as well as other structures [8]. Therefore, state-dependent survival and detection probabilities, $p_{S,k}(\cdot)$ and $p_{D,k}(\cdot)$, can enhance the tracking results. In our framework, we assume that these probabilities can be represented by Gaussian mixture models.

$$p_S(\acute{\xi}, \acute{r}) = w_S^{(0)}(\acute{r}) + \sum_{l=1}^{J_S(\acute{r})} w_S^{(l)}(\acute{r}) \mathcal{N}\left(F(r)\acute{\xi}; \mu_S^{(l)}(\acute{r}), \Sigma_S^{(l)}(\acute{r})\right), \quad 0 \leq p_S(\acute{\xi}, \acute{r}) \leq 1 \quad \forall \acute{\xi}, \acute{r} \quad (8)$$

$$p_D(\xi, r) = w_D^{(0)}(r) + \sum_{l=1}^{J_D(r)} w_D^{(l)}(r) \mathcal{N}\left(\xi; \mu_D^{(l)}(r), \Sigma_D^{(l)}(r)\right), \quad 0 \leq p_D(\xi, r) \leq 1 \quad \forall \xi, r. \quad (9)$$

The parameters of the survival and detection probabilities such as $w_S^{(l)}(\cdot), J_S(\cdot), \mu_S^{(l)}(\cdot), \Sigma_S^{(l)}(\cdot), w_D^{(l)}(\cdot), J_D(\cdot), \mu_D^{(l)}(\cdot)$ and $\Sigma_D^{(l)}(\cdot)$ are set based on the application.

Modeling birth term: In most of the previous applications, the locations of spontaneous births are either unknown or uniformly distributed everywhere in the image background [1, 6–8]. However in this filtering framework, a prior on birth locations is required to estimate the birth intensity distribution. To address this, we use a Gaussian term with very high variance, as the birth intensity distribution of the state ξ such that $\tilde{\gamma}(\xi) = w_\gamma \mathcal{N}(\xi; \mu_\gamma, \Sigma_\gamma)$, where w_γ represents the expected number of new born structures. This allows that any detected measurement has the same chance to be detected as new born targets. The birth intensity distribution for the augmented state $x = (\xi, r)$ is then given by $\gamma(\xi, r) = \tilde{\gamma}(\xi)\pi_\gamma(r)$, where $\pi_\gamma(r)$ is the probability of birth for model r [13].

A closed-form PHD recursion: Our model differs from Pasha *et al.* [13] by the introduction of state-dependent models for $t(\cdot|\cdot)$ and $\pi(\cdot|\cdot)$. Therefore, the closed-form for the predicted intensity $v_{k|k-1}(\cdot)$ will be different from [13]. However, the updated intensity $v_k(\cdot)$ are obtained similar to the general closed-form proposed in their paper. In order to show that there is a closed-form for the predicted intensity (Eq. 1) using the above models, two Lemmas are required:

Lemma 1: The product of a Gaussian and a conditional Gaussian has a weighted Gaussian form such that $\mathcal{N}(x; \mu, \Sigma)\mathcal{N}(z; Hx + d, R) = \lambda_b \mathcal{N}(x; \mu_b, \Sigma_b)$, where $\lambda_b = \mathcal{N}(z; H\mu + d, R + H\Sigma H^T)$, $\mu_b = \mu + K(z - d - H\mu)$, and $\Sigma_b = (I - KH)\Sigma$, where $K = \Sigma H^T(H\Sigma H^T + R)^{-1}$.

Lemma 2: The product of two Gaussian distributions is a weighted Gaussian such that $\mathcal{N}(x; \mu_1, \Sigma_1)\mathcal{N}(x; \mu_2, \Sigma_2) = \lambda_c \mathcal{N}(x; \mu_c, \Sigma_c)$, where $\lambda_c = \mathcal{N}(\mu_1; \mu_2, \Sigma_1 + \Sigma_2)$, $\Sigma_c = (\Sigma_1^{-1} + \Sigma_2^{-1})^{-1}$ and $\mu_c = \Sigma_c(\Sigma_1^{-1}\mu_1 + \Sigma_2^{-1}\mu_2)$.

According to Eq. 1, the $v_{k|k-1}(\cdot)$ is composed of three terms including intensity distributions due to existing targets $v_f(\cdot)$, spawned targets $v_\beta(\cdot)$ and spontaneous births $v_\gamma(\cdot)$ as $v_{k|k-1}(x) = v_f(x) + v_\beta(x) + v_\gamma(x)$. Supposing that the posterior intensity v_{k-1} at time $k - 1$ has a Gaussian mixture form

$$v_{k-1}(\dot{x}) = v_{k-1}(\dot{\xi}, \dot{r}) = \sum_{i=1}^{J(\dot{r})} w^{(i)}(\dot{r}) \mathcal{N}\left(\dot{\xi}; \mu^{(i)}(\dot{r}), \Sigma^{(i)}(\dot{r})\right), \quad (10)$$

and by substituting Eqs. 3, 8 and 10 into the first term of Eq. 1 and using Lemmas 1 and 2, it can be shown that $v_f(\cdot)$ has Gaussian mixture form,

$$v_f(\xi, r) = \sum_{\dot{r}} \sum_{i=1}^{J(\dot{r})} \sum_{l=0}^{J_S(\dot{r})} \sum_{j=0}^{J_t(r, \dot{r})} w_f^{(i,l,j)}(r, \dot{r}) \mathcal{N}\left(\xi; \mu_f^{(i,l,j)}(r, \dot{r}), \Sigma_f^{(i,l,j)}(r, \dot{r})\right). \quad (11)$$

The equations for $w_f^{(i,l,j)}$, $\mu_f^{(i,l,j)}$ and $\Sigma_f^{(i,l,j)}$ can be easily calculated using the aforementioned lemmas and we omit them here due to space restrictions. Similarly by substituting Eqs. 5 and 10 into the second term of Eq. 1 and using Lemmas 1 and 2, it can be shown that $v_\beta(\cdot)$ also has a Gaussian mixture form given by

$$v_\beta(\xi, r) = \sum_{\dot{r}} \sum_{i=1}^{J(\dot{r})} \sum_{j=1}^{J_\beta(r, \dot{r})} \sum_{l=0}^{J_\pi(r, \dot{r})} w_\beta^{(i,j,l)}(r, \dot{r}) \mathcal{N}\left(\xi; \mu_\beta^{(i,j,l)}(r, \dot{r}), \Sigma_\beta^{(i,j,l)}(r, \dot{r})\right). \quad (12)$$

As above, equations for $w_\beta^{(i,j,l)}$, $\mu_\beta^{(i,j,l)}$ and $\Sigma_\beta^{(i,j,l)}$ can be calculated using the lemmas. Finally, the last term in Eq. 1 is Gaussian term equal to

$$v_\gamma(\mathbf{x}) = \gamma(\xi, r) = w_\gamma \pi_\gamma(r) \mathcal{N}(\xi; \mu_\gamma, \Sigma_\gamma). \quad (13)$$

Consequently, $v_{k|k-1}(\cdot)$, which is sum of Eqs. 11, 12 and 13, is a Gaussian mixture. The closed-form suggested here for $v_{k|k-1}(\cdot)$ is more general than what is proposed in [13] and is applicable for an enhanced particle tracking in biological applications where the transition probability $t(\cdot|\cdot)$, the spawned transition probability $\pi(\cdot|\cdot)$ and survival and detections probabilities, $p_S(\cdot|\cdot)$ and $p_D(\cdot|\cdot)$, are state-dependant functions. The proposed scheme, however, is completely general and supports simpler models where some or all of these terms are state-independent.

Tag propagation scheme: In the PHD filtering framework, the identity of trajectories is not considered in the filter recursions and thus, the dynamics of an individual target cannot be evaluated. A method for propagating the identity of the tracks in Gaussian mixture probability hypothesis density (GM-PHD) filter is proposed in [17]. However, the method uses a heuristic technique to find the identity of crossing targets that is only applicable for the GM-PHD filter. Here, we propose a better solution for propagating track identities and solving crossing targets. Our solution applies to both GM-PHD and LGJMS-PHD filters. Supposing the identity of each Gaussian term in the posterior intensity v_{k-1} is known, the tags are propagated in our framework as follows.

Prediction step: The Gaussian terms in $v_f(\cdot)$ keep the identities of their parents v_{k-1} as these terms are related to existing targets which move based on their dynamics. For each Gaussian term spawned by an existing term with index i in the spawned term $v_\beta(\cdot)$, a new tag is assigned. For Gaussian terms introduced by the birth model, no tag is assigned in this step.

Update step: The Gaussian terms with existing identities, initially keep their tags after the update step. For each updated Gaussian term introduced by the birth model, a new tag is assigned in this step. This idea is based on the assumption that each generated measurement is either due to the targets or clutter and a single target cannot generate more than one measurement at each time frame.

Next, the state estimation procedure (i.e. thresholding on Gaussian terms) [14] is applied to revise the tags. Noting that an existing target cannot have more than one state at each time frame, if multiple target states are assigned with Gaussian terms having identical tags, the term with the highest weight keeps its identity and the remaining terms are assigned by a new tag.

A solution for crossing targets: From the PHD recursion, it can be seen that the number of intensity components increases as time progresses. Therefore, this filter is usually followed by a pruning step that eliminates and merges Gaussian terms [13, 14]. This step is applied to decrease computational burden and remove unlikely intensity distributions. However, it leads to identity loss in crossing targets. To avoid this, we simply suggest that merging between intensity terms can be performed only if their tags are identical. More precisely, the merging for the Gaussian terms with the different tags is not allowed in this approach.

4 Experimental results

We applied the proposed scheme for multi-target tracking in 2-D Total Internal Reflection Fluorescence Microscopy (TIRFM) sequences. TIRFM is an imaging technique that enables the selective excitation of fluorescently tagged proteins within a few hundred nanometers of the plasma membrane of a cell. This selective excitation characteristic of TIRFM has made it an ideal imaging technique for visualizing subcellular structures such as vesicles that are on or close to the plasma membrane [18]. The vesicles are very tiny subcellular structures and are seen in TIRFM sequences as small bright spots moving with different dynamics while appearing or disappearing from the field of view or are occluded by or spawned from other structures. Moreover, due to limitations in TIRFM acquisition process, the sequences are contaminated with a high level of noise [19].

We modeled the state of each vesicle by its position, $x = (x_x, x_y)$, and velocity, $\dot{x} = (\dot{x}_x, \dot{x}_y)$. The measurements $z = (\hat{x}_x, \hat{x}_y)$ were provided by the detection scheme proposed by Rezatofghi *et al.* [19]. Then, we applied our LGJMS-PHD filter using two linear dynamic models including random walk and small acceleration motion model [1, 3, 6]. The transition probability $t(\cdot|\cdot)$ were defined similar to the function suggested in [1]. This function can be easily represented as an affine mixture of Gaussians. Since the vesicles are spawned independently from the state of their parents, a state independent form of the spawned transition probability was used in this application $\pi(r|\dot{r}, \xi) = \pi(r|\dot{r})$. Moreover, $p_S(\cdot)$ in this current implementation is independent of the state of targets $p_S(\xi, \dot{r}) = p_S(\dot{r})$.

Since the main source of noise in this imaging technique is an intensity dependent noise (Poisson noise) [6], the signal to noise ratio (SNR) in the areas with higher intensity levels is lower. Therefore, the vesicles located in this area have lower detection probability. To improve the probability of detection, we defined it as a Gaussian mixture function of the target positions, x . Since the locations where spontaneous births may occur is unknown in this application, the birth intensity distribution is set as Gaussian distribution centered on the image with very high standard deviation.

Evaluation on realistic synthetic data: Due to complexity of the data, there is no reliable manual ground truth on the TIRFM sequences. To quantitatively evaluate the proposed tracking algorithm, it was first evaluated using realistic synthetic sequences generated by the framework proposed in [20]. The sequences simulated using this framework appropriately reflect the difficulties existing in real TIRFM sequences while providing accurate ground truth.

Moreover, we quantitatively compared the results of our LGJMS-PHD filter against the result of the IMM-JPDA filter proposed in [1]. Since this filter is a combination of a multiple model Bayesian filter and a very robust data-association technique, it is the most relevant traditional Bayesian tracking filter for comparison with our framework. In addition, our results are also compared against the result of the previously implemented LGJMS-PHD filter [13] when the $t(\cdot|\cdot)$, $\pi(\cdot|\cdot)$, $p_S(\cdot|\cdot)$ and $p_D(\cdot|\cdot)$ are independent of target state. To maximize the validity of our experiments, we chose identical parameters and models such as the same state vector, clutter rate, measurements and dynamic models, for

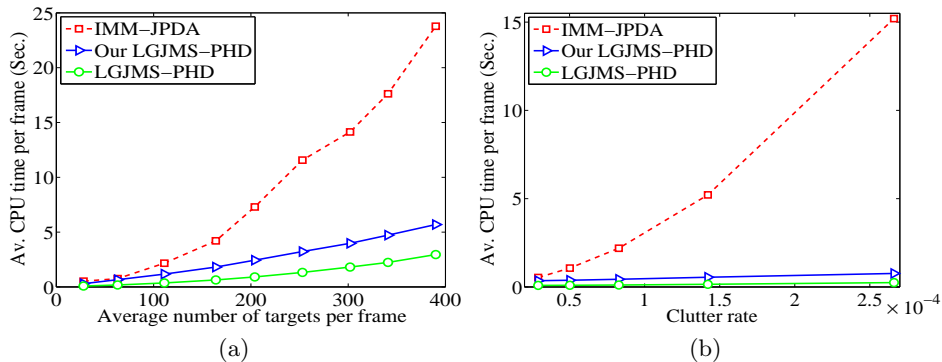


Fig. 1. The average CPU time per frame required for tracking the targets using the IMM-JPDA, the previous LGJMS-PHD and the proposed LGJMS-PHD filters in sequences with (a) different target densities and a constant clutter rate and (b) different clutter rate and a fixed average number of targets.

all filters. For other parameters which are not in common, we attempted to find the values that resulted in the best performance for the competing models.

In the first experiment, we compared the processing time required for these filters to track different numbers of targets in a fixed clutter rate. Here, clutter rate (λ_c) is defined as the average number of false measurements per pixel per frame. In Fig. 1(a), we see the both LGJMS-PHD filters require noticeably lower processing time for tracking large number of targets. However, since our LGJMS-PHD filter propagates more Gaussian terms for each target in each recursion, its processing time is higher than the time required for the original LGJMS-PHD filter. In the second experiment, we evaluated the performance of the tracking filters in different clutter rates but a fixed average number of targets. Fig. 1(b) shows that the processing time for the both LGJMS-PHD filters is significantly less than the IMM-JPDA filter.

To qualitatively assess the performance of these tracking methods, we used a metric based on optimal subpattern assignment (OSPA) [21]. This metric is the sum of two errors: cardinality and location. The cardinality error is related to missed or false tracks while location error shows track accuracy error and labeling error. In Table 1, the performance of these tracking filters is compared using this metric. To this end, we applied the filters for tracking targets in synthetic sequences including on average 164 targets per frame and clutter rate $\lambda_c = 1.01 \times 10^{-4}$. According to the table, the overall tracking performance for our LGJMS-PHD filter using this metric is better than the other filters. Compared to the previous LGJMS-PHD filter, this is an expected result as we have a better model for the $t(\cdot|\cdot)$ and $p_D(\cdot|\cdot)$.

In comparison with the IMM-JPDA filter, the both PHD filters have slightly higher location error. This is mostly due to labeling error in very hard scenarios such as several crossing targets with maneuvering dynamics. Intuitively, JPDA uses joint probability association of measurements to update the tracks while the PHD filters use the first statistical moment of this joint probability. Thus, the

Method	Location error	Cardinality error	OSPA
IMM-JPDA filter [1]	3.70	3.53	7.23
LGJMS-PHD [13]	3.98	2.12	6.10
Our LGJMS-PHD	3.92	1.80	5.72

Table 1. Comparison of the performance of the IMM-JPDA, the previous LGJMS-PHD filter and our LGJMS-PHD filters using OSPA metric [21] (lower value is better).

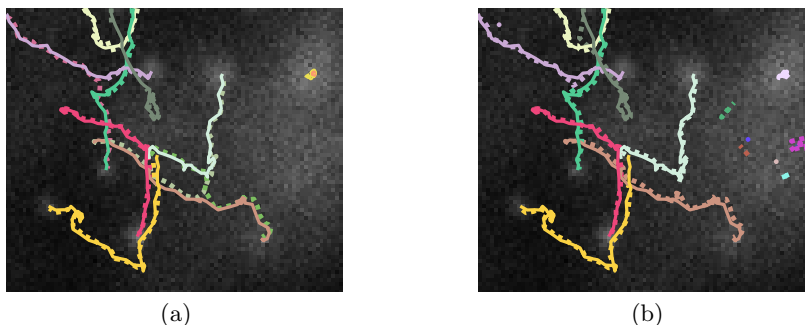


Fig. 2. An example where the PHD filter fails to accurately track several crossing targets with maneuvering motions. The ground truth (solid line) and tracking results (dashed line) for (a) our LGJMS-PHD and (b) the IMM-JPDA filters. The results of the PHD and IMM-JPDA filters include some labeling errors and false tracks, respectively.

PHD filters can not work as well as the IMM-JPDA filter in these cases (Fig. 2). In addition, the primary weakness of the PHD recursion is a loss of higher order cardinality information which causes noisy tracks specially when the density of targets are very high [22]. Therefore, this also affects track accuracy and increases the location error. In contrast, both PHD filters have the lower cardinality error compared to the IMM-JPDA filter due to less false and missed tracks. This is due to incorporating new born targets and clutter models in their recursions while there is no principled formulation for the IMM-JPDA filter. Fig. 2(b) shows that the result of the IMM-JPDA filter includes several false tracks which do not exist in the result of our PHD filter (Fig. 2(a)).

Evaluation on real data: The three tracking filters were also tested on real TIRFM sequences. Because manual delineation of trajectories for generating reliable ground truth for our data is an arduous and subjective task, the results of the tracking were visually assessed by an expert. The real sequences include about 300 targets per frame moving through a cell membrane with an effective region size of 200×210 pixels.

In this data, there are particles that are barely visible. To detect and track these particles, the threshold in the detection method should be set low. This increases clutter rate which dramatically increases the processing time and also the number of false tracks in the IMM-JPDA filter. In contrast, the proposed LGJMS-PHD filter allows us to track a significantly larger number of faint vesicles while keeping false track rate low with significantly lower processing time compared to the IMM-JPDA filter. However, the tracks resulted from the PHD filters are slightly noisy as previously mentioned. Furthermore, they have more

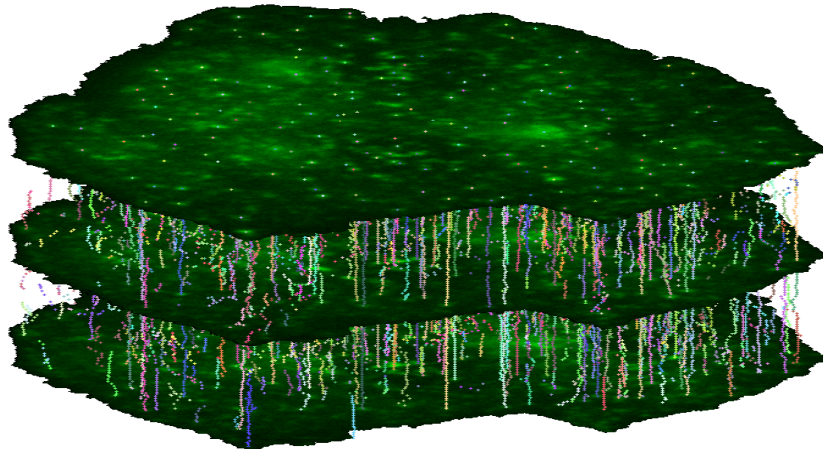


Fig. 3. Tracking result of our LGJMS-PHD filter for 100 real TIRFM sequences.

labeling errors in very hard scenarios where there are many crossing targets with different dynamics.

5 Conclusion

In this paper, we proposed a new closed-form recursion for the LGJMS-PHD filter by incorporating state-dependent transition probability matrix $t(\cdot|\cdot)$ and the spawned transition probability $\pi(\cdot|\cdot)$. This new closed-form is more general than what was proposed previously in the literature and therefore, allows more accurate PHD trackers for biological applications. Compared to traditional Bayesian trackers such as IMM-JPDA, the proposed filter has noticeably lower processing time in the cases where there are numerous targets and noisy detections. Therefore, it can be an accurate particle tracker in these applications especially when the number of crossing targets with maneuvering motions is reasonably restricted. In addition, our filter can properly detect and track spawned particles which is not well-principled in other traditional Bayesian filters. The main weakness of the PHD filters, including ours, is that they generate noisy trajectories in area with very high target density. To address this problem, we plan to use an improved version of the PHD filter, so called cardinalized PHD (CPHD) filter [22], in our future work.

References

1. Rezatofghi, S.H., Gould, S., Hartley, R., Mele, K., Hughes, W.: Application of the IMM-JPDA filter to multiple target tracking in total internal reflection fluorescence microscopy images. *MICCAI (2012)* 357–364
2. Yang, L., Qiu, Z., Greenaway, A., Lu, W.: A new framework for particle detection in low-SNR fluorescence live-cell images and its application for improved particle tracking. *IEEE Trans. Biomed. Eng.* **59**(7) (2012) 2040–2050

3. Feng, L., Xu, Y., Yang, Y., Zheng, X.: Multiple dense particle tracking in fluorescence microscopy images based on multidimensional assignment. *J. Struct. Biol.* **173**(2) (2011) 219–228
4. Yuan, L., Zheng, Y.F., Zhu, J., Wang, L., Brown, A.: Object tracking with particle filtering in fluorescence microscopy images: Application to the motion of neurofilaments in axons. *IEEE Trans. Med. Imag.* **31**(1) (2012) 117–130
5. Godinez, W., Lampe, M., Wörz, S., Müller, B., Eils, R., Rohr, K.: Deterministic and probabilistic approaches for tracking virus particles in time-lapse fluorescence microscopy image sequences. *Med. Image Anal.* **13**(2) (2009) 325–342
6. Smal, I., Meijering, E., Draegestein, K., Galjart, N., Grigoriev, I., Akhmanova, A., Van Royen, M., Houtsmuller, A., Niessen, W.: Multiple object tracking in molecular bioimaging by rao-blackwellized marginal particle filtering. *Med. Image Anal.* **12**(6) (2008) 764–777
7. Smal, I., Draegestein, K., Galjart, N., Niessen, W., Meijering, E.: Particle filtering for multiple object tracking in dynamic fluorescence microscopy images: Application to microtubule growth analysis. *IEEE Trans. Med. Imag.* **27**(6) (2008)
8. Wood, T., Yates, C., Wilkinson, D., Rosser, G.: Simplified multitarget tracking using the PHD filter for microscopic video data. *IEEE Trans. Circ. Syst. Vid.* **22**(5) (2012) 702–713
9. Juang, R., Levchenko, A., Burlina, P.: Tracking cell motion using GM-PHD. In: *Proc. ISBI.* (2009) 1154–1157
10. Vo, B.N., Singh, S., Doucet, A.: Sequential monte carlo methods for multitarget filtering with random finite sets. *IEEE Trans. Aerosp. Electron. Syst.* **41**(4) (2005)
11. Mahler, R.: Multitarget bayes filtering via first-order multitarget moments. *IEEE Trans. Aerosp. Electron. Syst.*, **39**(4) (2003) 1152–1178
12. Maggio, E., Taj, M., Cavallaro, A.: Efficient multitarget visual tracking using random finite sets. *IEEE Trans. Circ. Syst. Vid.* **18**(8) (2008) 1016–1027
13. Pasha, S., Vo, B.N., Tuan, H., Ma, W.: A gaussian mixture PHD filter for jump markov system models. *IEEE Trans. Aerosp. Electron. Syst.* **45**(3) (2009) 919–936
14. Vo, B.N., Ma, W.: The gaussian mixture probability hypothesis density filter. *IEEE Trans. Signal Process.* **54**(11) (2006) 4091–4104
15. Keller, P., Pampaloni, F., Lattanzi, G., Stelzer, E.: Three-dimensional microtubule behavior in xenopus egg extracts reveals four dynamic states and state-dependent elastic properties. *Biophys. J* **95**(3) (2008) 1474–1486
16. Cohen, A., Gomes, F., Roysam, B., Cayouette, M.: Computational prediction of neural progenitor cell fates. *Nature methods* **7**(3) (2010) 213–218
17. Panta, K., Clark, D., Vo, B.N.: Data association and track management for the gaussian mixture probability hypothesis density filter. *IEEE Trans. Aerosp. Electron. Syst.* **45**(3) (2009) 1003–1016
18. Burchfield, J., Lopez, J., Mele, K., Vallotton, P., Hughes, W.: Exocytotic vesicle behaviour assessed by total internal reflection fluorescence microscopy. *Traffic* **11** (2010) 429–439
19. Rezatofghi, S.H., Hartley, R., Hughes, W.: A new approach for spot detection in total internal reflection fluorescence microscopy. In: *Proc. ISBI.* (2012) 860–863
20. Rezatofghi, S.H., Pitkeathly, W., Gould, S., Hartley, R., Mele, K., Hughes, W., Burchfield, J.: A framework for generating realistic synthetic sequences of total internal reflection fluorescence microscopy images. In: *Proc. ISBI.* (2013)
21. Ristic, B., Vo, B.N., Clark, D., Vo, B.T.: A metric for performance evaluation of multi-target tracking algorithms. *IEEE Trans. Signal Process.* **59**(7) (2011)
22. Vo, B.T., Vo, B.N., Cantoni, A.: Analytic implementations of the cardinalized probability hypothesis density filter. *IEEE Trans. Signal Process.* **55**(7) (2007)